



Contents lists available at ScienceDirect

## Arabian Journal of Chemistry

journal homepage: [www.ksu.edu.sa](http://www.ksu.edu.sa)

# Analysis of water adsorption capacity and thermal behavior of porous carbonaceous materials by glycerol ester

Ziting Gao<sup>a,1</sup>, Lu Han<sup>b,1</sup>, Jiqiang Wan<sup>b,1</sup>, Guangming Fu<sup>a,1</sup>, Xiaopeng Yang<sup>a</sup>, Qi Guo<sup>c</sup>, Xiaoming Ji<sup>a,\*</sup>, Wenjuan Chu<sup>b,\*</sup>, Haiying Tian<sup>b,\*</sup>, Miao Lai<sup>a,\*</sup>

<sup>a</sup> Flavors and Fragrance Engineering & Technology Research Center of Henan Province, College of Tobacco Science, Henan Agricultural University, Zhengzhou 450046, China

<sup>b</sup> Technology Center of China Tobacco Henan Industry Co., Ltd, Zhengzhou 450000, China

<sup>c</sup> Henan Province Xinzheng Jinye Perfume Co. Ltd, Flavors and Fragrance Engineering & Technology Research Sub-Center of Henan Province, Zhengzhou 451100, China

## ARTICLE INFO

## Keywords:

Glycerol esters  
Moisture property  
LF-NMR  
Py-GC/MS  
Thermal behaviors

## ABSTRACT

The addition of glycerol, a traditional humectant, during the storage of reconstituted tobacco accelerated the deterioration of product quality due to the excessive absorption of moisture from the air by the tobacco and glycerol, which have strong hygroscopic properties. Therefore, it is crucial to develop a new humectant with moderate moisture resistance properties. In this study, a series of compounds glycerol esters were synthesized by transesterification reaction with vinyl benzoate and vinyl cinnamate via Novozym 435 using glycerol as a starting material. Nuclear magnetic resonance (<sup>1</sup>H NMR, <sup>13</sup>C NMR), infrared spectroscopy (IR), and high resolution mass spectrometry (HRMS) were used to confirm the structure of synthesized glycerol esters. The target compounds were added to the reconstituted tobacco shreds for 100 h hygroscopic desorption assay, model validation, moisture proof index and moisture retention index. The hygroscopicity and moisturizing ability was assessed using water activity and low-field nuclear magnetic resonance (LF-NMR). It showed that 3a (2,3-dihydroxypropyl benzoate) and 3b (2,3-dihydroxypropyl cinnamate) possessed better moisture absorption and moisturizing effect. In addition, thermogravimetric analysis (TG) and pyrolysis-gas chromatography/mass spectrometry (Py-GC/MS) techniques were applied to study the thermal behavior of 3a and 3b. These results indicated that the target compounds (3a and 3b) had good moisture absorption and moisture retention effects, high temperature stability and thermal properties for flavour release. They could effectively improve the water absorption, enhance the flavour of reconstituted tobacco, and were suitable for use in the storage and smoking process of reconstituted tobacco.

## 1. Introduction

Tobacco as one of the special economic crops has been widely noticed and studied (Huang et al., 2021). Heated non-burning cigarette (HNB) is a new type of tobacco product that usually below 350 °C to create smoke for consumer inhalation (Lachenmeier, Anderson & Rehm, 2018), producing an aerosol with fewer toxic substances than traditional tobacco products (Simonacicius et al., 2019). Since reconstituted tobacco is a porous carbohydrate material, the storage environment and relative humidity of the air can easily affect the change of its moisture

content (Yin et al., 2015), which has a greater impact on the quality of heated non-combustible tobacco products (Samejima, Soh & Yano, 1978). It not only affects the processing characteristics of heated non-combustible tobacco products but also negatively affects the smoking quality and shelf life (Mutasa, Seal, & Magan, 1990; Samejima & Yano, 1985; IH & GR, 2014).

Since the hydroxyl group of the traditional moisturizing agent glycerol can generate hydrogen bonding force with water molecules (Zhou et al., 2016), which has the effect of moisturization, the addition of glycerol during the production of reconstituted tobacco can

\* Corresponding authors at: Flavors and Fragrance Engineering & Technology Research Center of Henan Province, College of Tobacco Science, Henan Agricultural University, No. 218, Ping'an Avenue, Zhengdong New District, Zhengzhou 450046, PR China (X. Ji and M. Lai). And Technology Center of China Tobacco Henan Industry Co., Ltd, No. 8 Jingkai Third Street, Guancheng Hui Ethnic District, PR China (W. Chu and H. Tian).

E-mail addresses: [xiaomingji@henau.edu.cn](mailto:xiaomingji@henau.edu.cn) (X. Ji), [chuwenjuan6@126.com](mailto:chuwenjuan6@126.com) (W. Chu), [haiyingflying@163.com](mailto:haiyingflying@163.com) (H. Tian), [laimiao@henau.edu.cn](mailto:laimiao@henau.edu.cn) (M. Lai).

<sup>1</sup> These authors contributed equally to this study and share first authorship.

<https://doi.org/10.1016/j.arabjc.2024.105789>

Received 24 September 2023; Accepted 6 April 2024

Available online 8 April 2024

1878-5352/© 2024 The Authors. Published by Elsevier B.V. on behalf of King Saud University. This is an open access article under the CC BY-NC-ND license (<http://creativecommons.org/licenses/by-nc-nd/4.0/>).

effectively alleviate the water-loss characteristics of reconstituted tobacco, thus reducing the water loss in the tobacco (Heck et al., 2002; Rainey et al., 2013.). However, during the storage process of reconstituted tobacco with added glycerol, due to the strong hygroscopicity of glycerol itself, the tobacco is exposed to relatively high humidity (RH) for a long period of time. And the excessive moisture content will accelerate the deterioration of product quality or even mould. Therefore, it is important to develop a new type of moisture retention agent with moderate moisture retention properties.

For example, polysaccharides extracted from natural plants could improve the moisturizing effect of tobacco (Lin et al., 2020), our group had found that glycerol and flavored pyrrole derivatives as raw materials were synthesized by esterification to produce a new glycerol-ester moisturizer, which can also be used to enhance the flavour of tobacco while moisturizing the tobacco (Fan et al., 2023). Moreover, it has been reported that after splicing propylene glycol with flavour molecules to synthesize compounds, the strong hygroscopicity of the raw materials can be reduced and the flavour can be released by cracking at high temperatures (Gao et al., 2023). Benzoate and cinnamate esters are present in different flavours such as methyl cinnamate, ethyl cinnamate, butyl cinnamate, geranyl cinnamate, isoamyl cinnamate, benzyl cinnamate, etc. (Johnson et al., 2017; Cebrián-Tarancon et al., 2022; Xiang et al., 2020.), which are widely used in the field of cosmetics, food, pharmaceuticals, perfumery, as well as in the field of tobacco (Błaszczuk et al., 2021; Grajales-Hernández et al., 2021; Prakash, Singh, Mishra & Dubey, 2012; Gunia-Krzyzak et al., 2018).

As the traditional methods of extracting monomer flavours from plants naturally have high cost and low yield (Tani et al., 2019), chemical synthesis methods to increase the yield are accompanied by problems such as pollution of the environment and unsafety (Pan et al., 2019). In contrast, lipase as a catalyst for ester synthesis is in line with the green and safe theme and at the same time sustainable production (Wenda, Illner, Mell & Kragl, 2011). Low-Field Nuclear Magnetic Resonance (LF-NMR) is unaffected by changes in sample morphology, colour and size, and the technique is simple and stable (Ates, et al., 2021; Hu et al., 2018). This technology can be non-destructive, non-invasive through the change of transverse relaxation time  $T_2$  to real-time, rapid, intuitive monitoring and observation of the sample internal moisture distribution state to help from a microscopic point of view to analyse the pattern of change in the migration of the sample water (Wei et al., 2018; Yang et al., 2019).

To provide theoretical basis and key technologies for the development of moisturizing agents for heated non-combustible tobacco products, the synthesis of flavour molecular compounds with hydroxyl groups was carried out using Novozym 435 as a catalyst and transesterification reaction of glycerol with vinyl benzoate and vinyl cinnamate. Then evaluated the hygroscopicity and moisture retention, hygroscopicity and desorption model of the synthesized glycerol esters in reconstituted tobacco shreds. And determine the moisture presence state and distribution percentage of the reconstituted tobacco shreds by using LF-NMR. Two compounds were screened for better moisturizing effect as 3a (2-hydroxypropyl benzoate) and 3b (2-hydroxypropyl cinnamate), respectively. In addition, the thermal behavior and pyrolysis products of the screened glycerol esters were investigated using TG-DSC and Py-GC/MS.

## 2. Materials and methods

### 2.1. Materials and instruments

All the chemical substances and solvents employed in this study were of the commercial grade and acquired from Tianjin Kermel Chemical Reagent Co., Ltd. (China). In addition, the identification and confirmation of the structures of the novel target compounds were supported by instrumentation including the BRUKER/AVANCE NEO 400 MHz NMR spectrometer (BioSpin GmbH) utilizing  $CDCl_3$  as the solvent with

tetramethylsilane (TMS) as the internal standard, the advanced Fourier transform infrared spectrophotometer Nicolet iS50 (Thermo Nicolet Co, Waltham, MA, USA), and the Waters Micromass Q-TOF high-resolution mass spectrometer (Micro TM, Agilent, USA).

Reconstituted tobacco was supplied by Henan Cigarette Industry Tobacco Flake Co. Reconstituted tobacco has been cut into rectangular slices of uniform size, with a length of 28 cm and a width of 18 cm. Meanwhile, the moisture content of the reconstituted tobacco was 14 %.

### 2.2. Synthesis of glycerol esters

Under air conditions, the biological enzyme Novozym 435 (30 mg), glycerol (0.2 mmol) with vinyl carboxylate (1.0 mmol) was added to 2.5 mL of anhydrous acetonitrile and the mixture was fermented in a shaking water bath at 40 °C and 150 rpm for 36 h (Zhao et al., 2023). The completion of the reaction was monitored by TLC. After completion of the reaction, the bioenzymes were recovered by filtration and their liquid mixture was evaporated, added to ethyl acetate, subjected to column chromatography on silica gel (100 mesh) and eluted in a 10:1 petroleum ether/ethyl acetate solution to refine the crude residue, providing compounds 3a (60 % yield), 3b (63 % yield), 4a (15 % yield), 4b (14 % yield), and compounds 5a (13 % yield), 5b (13 % yield). The reaction route is shown below (Scheme 1).

### 2.3. Hygroscopicity and moisturizing

#### 2.3.1. Preparation of experimental samples

Firstly, the reconstituted tobacco leaves were shredded and passed through a 20 mesh sieve to remove the shreds, and the shredded tobacco was placed in a constant temperature and humidity chamber for 48 h at  $(22 \pm 1)$  °C and RH =  $(60 \pm 2)\%$  for equilibration. 20 mg of glycerides (3a, 4a, 5a, 3b, 4b, and 5b) were weighed separately and distilled water was added to make a solution of 1.2 % by mass. The glycerol ester solution was evenly sprayed on the surface of the reconstituted tobacco shreds until the content of glycerides reached 0.4 % of the total mass of the tobacco (5 g). In addition, reconstituted tobacco shreds sprayed with the same mass of glycerol and distilled water were used as a control group. The treated shredded reconstituted tobacco was again placed in a constant temperature and humidity chamber at  $(22 \pm 1)$  °C, RH =  $(60 \pm 2)\%$  for 72 h. The equilibrated shredded tobacco was divided into three groups, one of which was used to determine the initial moisture content of the shredded tobacco; meanwhile, the remaining two groups were respectively placed in a desiccator with solution containing saturated potassium chloride ( $(22 \pm 1)$  °C, RH =  $(84 \pm 2)\%$ ) and saturated magnesium chloride ( $(22 \pm 1)$  °C, RH =  $(32 \pm 2)\%$ ) for hygroscopic and desorption experiments (Fig. 1). Samples were removed at regular intervals and accurately weighed and recorded, and the moisture content of the samples at different times was calculated based on the moisture changes during storage (Fan et al., 2023; Gao et al., 2023).

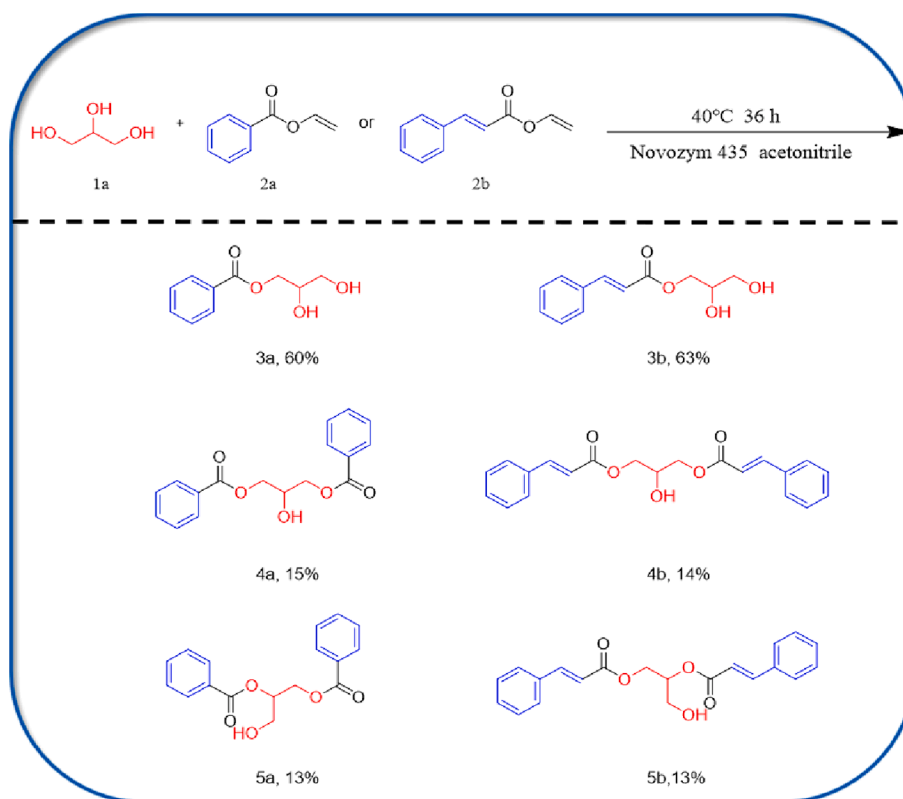
#### 2.3.2. Model evaluation methods

The dry basis moisture content of tobacco shred was converted into the moisture ratio  $MR$  according to Formula (1).

$$MR = \frac{M_t - M_e}{M_0 - M_e} \quad (1)$$

where the  $M_e$  was dry equilibrium basis moisture content (%),  $M_t$  was dry basis moisture content at  $t$  h (%),  $M_0$  was initial dry basis moisture content (%).

A few models related to adsorption and desorption have been proposed. In this study the experimental data were matched to the origin programmer, different models were fitted to the  $MR-t$  data using a non-linear fit, (version 19.0, OriginLab Inc., Northampton, MA, USA). The coefficient of determination ( $R^2$ ) and root mean square error (RMSE) were calculated to assess the model fitting results. Where, the closer  $R^2$  is



**Scheme 1.** The range of substrates in the esterification reaction between glycerol and vinyl carboxylate.

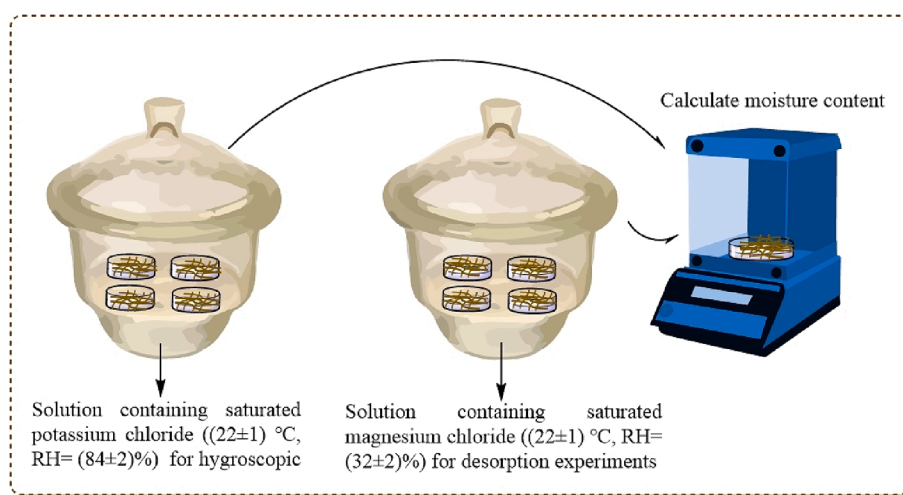


**Fig. 1.** Tobacco shred added with different polyol materials in different RH.

to 1, the smaller the root mean square error (*RMSE*) is and the more reliable the model is.  $R^2$  and *RSME* were calculated according to Formulas (2) and (3), respectively.

$$R^2 = \frac{\sum_i^N (MR_{pre,i} - \overline{MR}_{exp,i})^2}{\sum_i^N (MR_{exp,i} - \overline{MR}_{exp,i})^2} \quad (2)$$

$$RMSE = \left[ \frac{1}{N} \sum_i^N (MR_{pre,i} - MR_{exp,i})^2 \right]^{\frac{1}{2}} \quad (3)$$

where  $N$  is the number of experimental observations,  $MR_{exp}$  is the moisture ratio test value, and  $MR_{pre}$  is the moisture ratio model

prediction.

### 2.3.3. Establishment of dynamic model

Three common models (Page, Wang and Singh and Henderson-Pabis) were selected to simulate the moisture absorption and desorption processes of reconstructed tobacco with different moisturizing agents, and the optimal models were screened out, and the commonly used kinetic models of tobacco are shown in Formulas (4)–(6).

$$\text{Page: } MR = \exp(-kt^n) \quad (4)$$

$$\text{Wang and Singh: } MR = at^2 + bt + 1 \quad (5)$$

$$\text{Henderson-Pabis: } MR = a \exp(-kt) \quad (6)$$

where  $t$  is the hygroscopic or desorption time,  $k$ ,  $n$ ,  $a$  and  $b$  are model parameters.

### 2.3.4. Calculation of the moisture protection index (MPI) and moisture retention index (MRI)

The obtained model parameters were used to calculate the half-life average hygroscopic/desorption rate  $v$  (%/h) and finally the MPI and MRI values.

$$v = \frac{|M_0 - M_e|/2}{t_{1/2}} \quad (7)$$

$$MPI = 4 - \frac{v}{\bar{v}} - \frac{M_e}{M_e} \quad (8)$$

$$MRI = 2 - \frac{v}{\bar{v}} + \frac{M_e}{M_e} \quad (9)$$

Where  $t_{1/2}$  is the half-life time ( $MR = 1/2$ , h);  $M_e$  is the arithmetic mean of  $M_e$  for each sample;  $v$  is the arithmetic mean of  $v$  for each sample.

### 2.3.5. LF-NMR analysis

Moisture state and ratio in tobacco shred was assessed by measuring the transverse relaxation time ( $T_2$ ) determined by PQ001MicroMR Cabinet NMR Imager (Shanghai Niumai Electronic Technology Co., Ltd.). The preparation of tobacco samples was consistent with Section 2.2.1. To attain constant weights, all samples were equilibrated under 22 °C with RH of 32 % and 84 %, respectively. 1.5 g of each group was weighed and put into the NMR sample tube (1 cm × 3.5 cm) for analysis and set up three parallel experiments. The CPMG pulse sequence was used to undertake data capture once the FID sequence had calibrated the resonant center frequency. The following were the CPMG sequence's parameters: probe coil diameter: 18 mm; magnet temperature: 32.00 ± 0.01 °C; resonance frequency (SF) = 22 MHz; offset frequency (O1) = 778183.37 Hz; pulse time (P1) = 21 μs; number of data points (TD) = 239994; repeated sampling waiting time (TW) = 5000.000 ms; pulse time (P2) = 40 μs; echo time (TE) = 0.300 ms; NECH = 8000; spectral width (SW) = 100 KHz; radio frequency delay (RFD) = 0.080 ms; analog gain (RG1) = 3 db; DR = 3; and NS = 32 echo time. Inversion of the  $T_2$  decay curve finally led to the observation of transverse relaxation time ( $T_2$ ) spectra.

### 2.3.6. Statistical analysis

Three independent experiments were conducted under the same conditions. A non-linear fit was performed using Origin 2019b.  $R^2$  and RMSE were used to assess the accuracy of the regression equations. Results were expressed as means using IBM's SPSS version 19.0 (Armonk, New York, USA) and significance was defined as  $P < 0.05$ .

## 2.4. Thermal behavior analysis

### 2.4.1. TG analysis

The thermogravimetric (TG) curves of the target compounds (STA 449 F3, Netzsch, Germany) were recorded using spectrally pure  $Al_2O_3$  as the reference material, which maintaining the mass of the target compound at approximately 5 mg at a time, an air atmosphere, maintaining a flow rate of 60 mL min<sup>-1</sup>, a heating rate of 10 °C min<sup>-1</sup> and a temperature range of 30–450 °C, respectively.

### 2.4.2. Pyrolysis analysis

Py-GC/MS analysis (Pyroprobe 5250T, CDS, Analytical Corporation, and Agilent 7890/5975, USA) was applied to identify the pyrolysis products of the target compounds. Approximately 2 mg of each sample was placed in a 25 mm quartz tube and fractured at a predetermined temperature for 10 s. The pyrolysis temperatures were set at 250 °C, 300 °C and 350 °C, respectively. The reactor was first heated at 6 °C min<sup>-1</sup>

and held at 50 °C. The tests were carried out in an air environment.

A capillary column DB-5MS (30 m × 250 μm × 0.25 μm) was used for the chromatographic separation. The predetermined inlet temperature was 300 °C. The oven was initially set at 50 °C and then ramped up to 80 °C at 6 °C min<sup>-1</sup> and then to 110 °C and held for 2 min. After 2 min, the oven reached a final temperature of 280 °C at a rate of 5 °C min<sup>-1</sup>. In the absence of splitting, helium was used as the carrier gas at a flow rate of 1 mL min<sup>-1</sup>.

The mass spectrometer checked the separated components. The transfer line was heated to 300 °C and the energy of the EI was fixed at 70 eV. The quadrupole temperature was 150 °C and the ion source temperature was specified at 230 °C. Mass spectra were collected from 30 to 500  $m/z$  with a solvent delay time of 2.8 min. A mass spectral library (NIST17) attached to the GC/MS instrument was used to match pyrolysis products.

## 3. Result and discussion

### 3.1. Characterization of target compounds

The structures of 3a, 4a, 5a, 3b, 4b, and 5b were characterized by <sup>1</sup>H and <sup>13</sup>C NMR shown in (Fig. 2a and b). The major signals of H atom in the benzene ring and CH=CH appeared in 8.05–6.30 ppm and corresponding signals of non-benzene ring H occurred in 4.49–0.89 ppm, respectively. The major signals of C atom in the benzene and O–C=O were in low field region, while the others moved in high field area.

The FTIR spectra of the series of target compounds were shown in (Fig. 2c). In the spectra, the peaks at 3410 cm<sup>-1</sup> and 3480 cm<sup>-1</sup> in target compounds corresponded to the telescopic vibrational absorption peaks of the structural –OH group, which is a typical functional group in the structure of glycerol. The synthesized compounds retained the characteristic absorption peaks of the benzene ring, indicating the successful synthesis of the series of target compounds. As shown in (Fig. 2d), the calculated value of  $m/z$  with Na added for 3a, 4a, 5a, 3b, 4b and 5b were 219.0628, 323.0890, 323.0890, 245.0784, 375.1203 and 375.1203 respectively, and that of find were 219.0620, 323.0906, 323.0884, 245.0777, 375.1212 and 375.1212.

### 3.2. Evaluation of hygroscopicity and moisturizing properties of target compounds

#### 3.2.1. Effect of target compounds on moisture retention and absorption of reconstituted tobacco shreds

The differences in hygroscopicity and humectancy of the resulting compounds were further investigated, respectively, and the results are shown in Fig. 3 (Fig. 3a and c, RH = 84 %), the good hydrophilicity of the humectants under high humidity conditions made the initial moisture content of the reconstituted tobacco filaments with humectants added higher than that of the blank filaments. In the process of humidification, the water content of the tobacco increased slowly in the first 20 h, and then increased linearly with time. Then gradually slowed down after 80 h, and finally reached equilibrium at 100 h. When equilibrium was reached, the dry-base water contents of tobacco with different humectants were in the following order from high to low: glycerol > 3a > 4a > 5a > blank control, glycerol > 3b > 4b > 5b > blank control. Their water content reached 81.94 %, 71.22 %, 52.58 %, 37.86 % and 23.77 %, 77.22 %, 66.90 %, 51.17 %, 45.95 % and 34.12 %, respectively.

As shown in (Fig. 3b and d), the moisture content of the tobacco samples at RH = 32 % decreased with the increase of desorption time, and all the samples showed almost the same decreasing trend in the first 6 h, and then equilibrium was reached at 100 h. Currently, the order of the shredded tobacco water content from high to low at this time is consistent with the results of the high humidity environment.

From Fig. 3, the humectancy and hygroscopicity of 3a and 3b were higher than that of the control, but lower than that of glycerol. This is

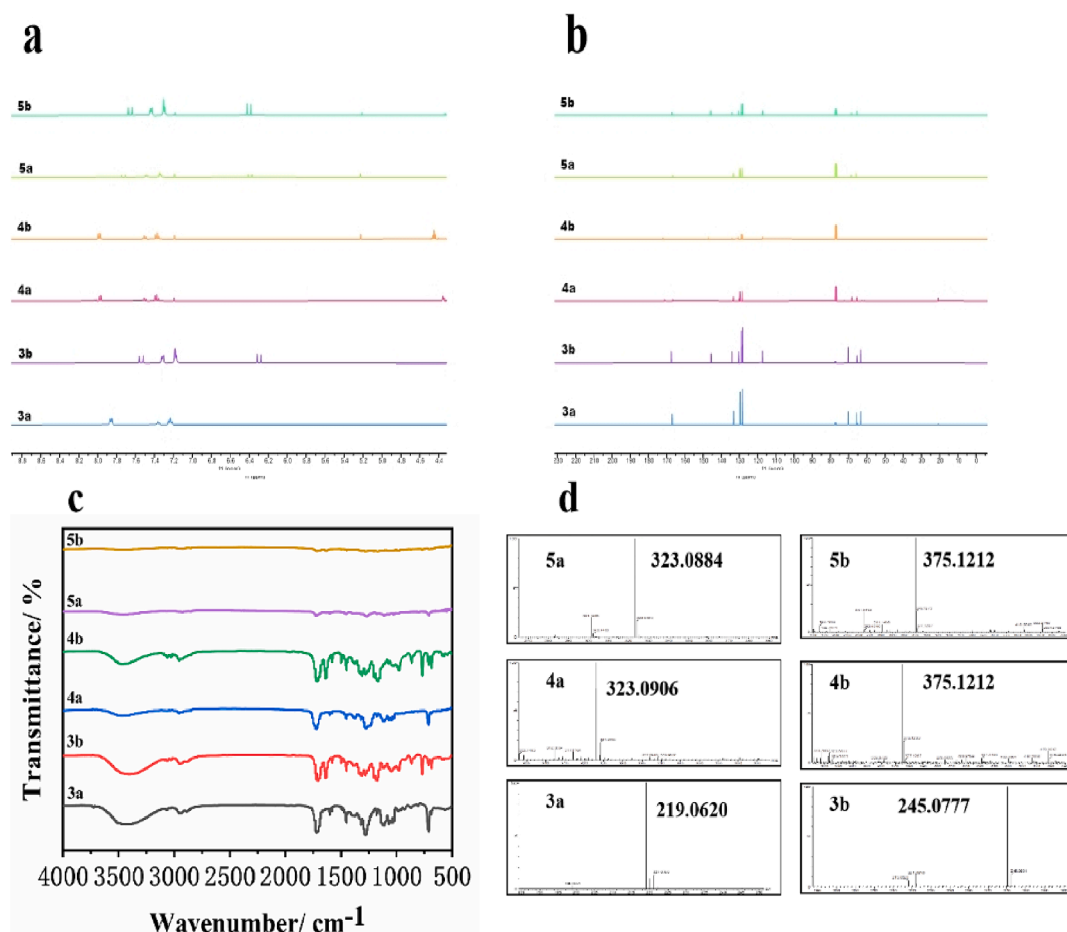


Fig. 2.  $^1\text{H}$  (a),  $^{13}\text{C}$  (b) NMR, FTIR (c), and HRMS (d) of target compounds.

because the strong hygroscopicity of glycerol can bind water molecules through hydrogen bonding, which enhances the affinity and adsorption capacity of shredded tobacco to water. Compared with glycerol, the number of hydroxyl groups in 3a and 3b was reduced, and the number of hydrogen bonds formed was consequently decreased. At the same time due to the hydrophobic effect of ester bonds, the water-absorbing ability of the tobacco was obviously weakened (Qin et al., 2002; Wang et al., 2013). As a result, it reduced the strong hygroscopicity of glycerol meanwhile it also had a certain degree of humidity-control and moisture-retaining ability.

### 3.2.2. Dynamic model of moisture absorption and desorption

Absorption and desorption models could be used to describe the relationship between time and the internal moisture ratio of the shredded tobacco. Tables 1 and 2 showed the fitting of three models and the corresponding  $R^2$  and RMSE values. From Table 1,  $R^2 > 0.90$  indicated that all three models were fitted well and the Page model having the largest  $R^2$  and the smallest RMSE, which had the best fitting effect. As shown in Table 2, the  $R^2$  of Page and Henderson-Pabis models was closest to 1, indicating that the fitting effect of these two models was better, among which the Page model had the best fitting effect and could better reflect the desorption process of shredded tobacco.

In summary, the Page model was the best model for both hygroscopic and desorption processes, with the highest model fit  $R^2$  up to 0.99313 and RMSE as low as 0.00104, demonstrating that the model could more accurately describe and predict the change rule of the moisture law (kinetic process) of reconstituted tobacco in different humidity environments.

### 3.2.3. Optimized model fitting parameters

Tables 3 and 4 showed the values of each set of constants calculated from Page model under different humidity environments. It was shown that the k-values of tobacco shreds samples were significantly different because of the characteristics of the humectants. And the values reflected the speed of water loss or absorption rate of a certain sample.

### 3.2.4. Evaluation of moisture proof index and moisture retention index of target compounds in reconstituted tobacco shreds

The curves were substituted into the Page model for nonlinear fitting, and the half-life mean moisture absorption/desorption rate ( $\nu$ ) was calculated according to the model parameters as the kinetic index, and the moisture protection index (MPI) and moisture retention index (MRI) were calculated as the comprehensive evaluation index.  $\nu$  represented the mean moisture absorption/desorption rate when the moisture change reached the midpoint ( $\text{MR} = 0.5$ ), and the smaller the value, the more stable the moisture of reconstituted tobacco was under the high or low humidity environments. Therefore, according to Eqs (7) and (8), the larger the values of MRI and MPI, the stronger the moisture retention and moisture resistance of the tobacco.

The  $\nu$ , MPI and MRI calculated from Page's model are shown in Table 5. During the moisture absorption process, the tobacco with the addition of glycerol had the largest  $\nu$  (0.7245 %/h) and the lowest MPI (0.8716). The results showed that glycerol could accelerate the rate of moisture absorption in reconstituted tobacco and the reason could be explained by the hydrogen bonding effect. The industry commonly applied large amounts of glycerol to reconstituted tobacco, which made its quality unstable in high humidity environments, and accelerated the deterioration of the quality of tobacco products during storage. The

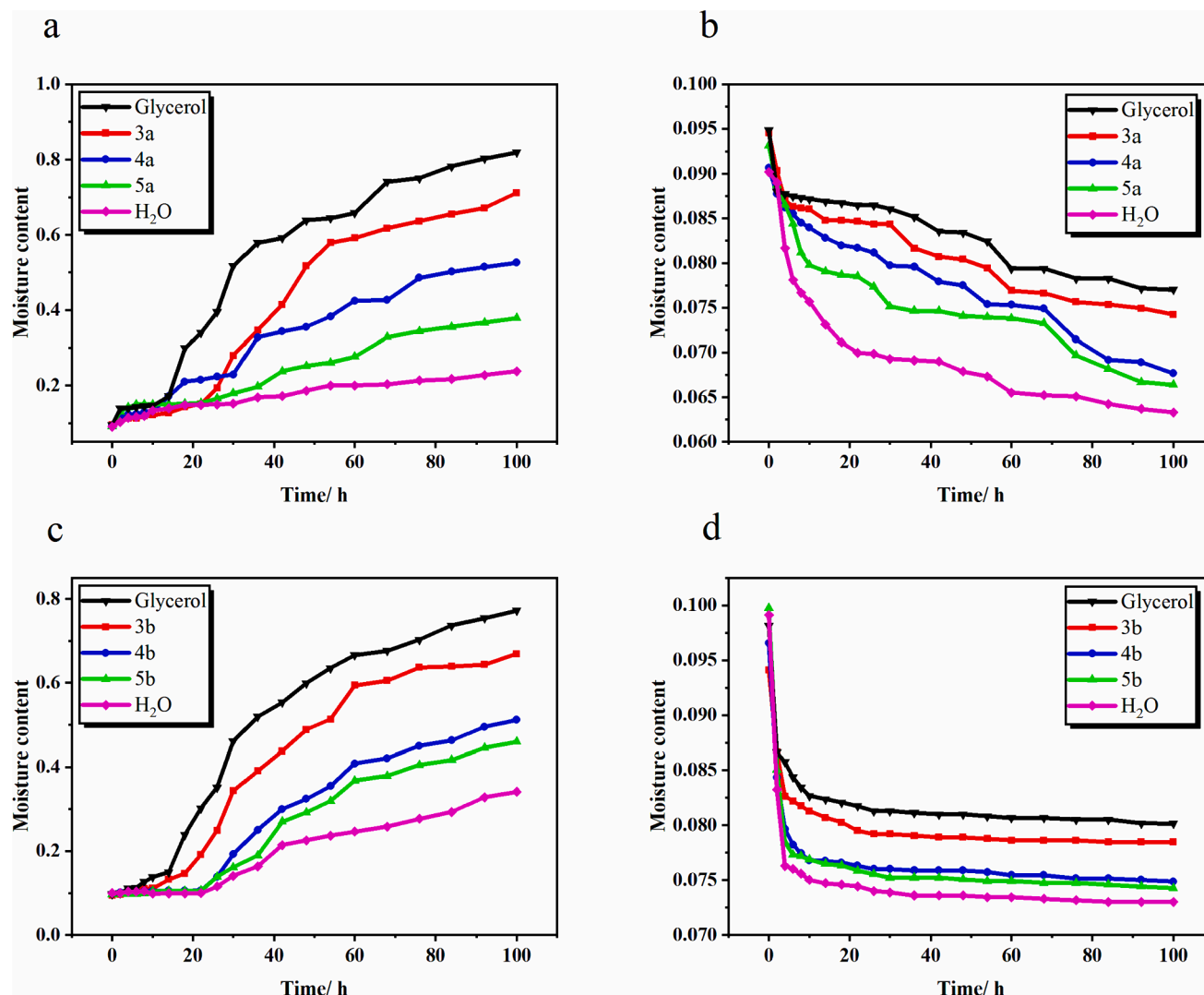


Fig. 3. The moisture contents of reconstituted tobacco shred at 22 °C, RH = 84 % (a, c); RH = 32 % (b, d).

Table 1

Fitting results of different models for moisture absorption of reconstituted tobacco shreds (RH = 84 %, 22 °C).

Sample	Page		Wang and Singh		Henderson-Pabis	
	R <sup>2</sup>	RMSE	R <sup>2</sup>	RMSE	R <sup>2</sup>	RMSE
Glycerol	0.98292	0.00222	0.96858	0.00407	0.96518	0.00272
3a	0.98802	0.00172	0.93146	0.00985	0.92418	0.00668
4a	0.98375	0.00182	0.98164	0.00155	0.93193	0.00281
5a	0.94752	0.00793	0.94197	0.00498	0.93651	0.00189
Control	0.94087	0.00558	0.9377	0.00732	0.90422	0.00524
Glycerol	0.98969	0.00148	0.96144	0.00553	0.96525	0.00441
3b	0.99313	0.00104	0.94106	0.00473	0.9673	0.00262
4b	0.98648	0.00188	0.94215	0.00445	0.93396	0.00508
5b	0.9896	0.00145	0.96439	0.00264	0.90927	0.00672
Control	0.97109	0.00339	0.90446	0.00616	0.91086	0.00409

average moisture absorption rates of the tobaccos shreds with synthetic glycerol esters were all less than that of glycerol under high humidity conditions, and the corresponding MPI were higher than that of the glycerol samples. Among them, sample 5a had the slowest moisture absorption rate of 0.2879 (%/h) and MPI of 2.6590.

On the contrary, during the desorption process, the average water loss rate ( $\nu$ ) of glycerol was lower than that of the other samples. Therefore, the glycerol-added tobacco shreds had the largest MRI. It

showed that the glycerol could improve the moisturizing properties of the tobacco shreds to a certain extent. The average moisture adsorption rates ( $\nu$ ) of the tobacco shreds with synthetic glycerol esters added were all lower than that of the blank and higher than that of the glycerol samples under low humidity conditions, and the corresponding MRI were higher than that of the blank but lower than that of the glycerol samples. The difference between MRI of 3a and 3b samples and glycerol samples was the smallest, reaching 2.0386 and 2.0459, respectively. This could be attributed to the hydrophobic effect of the ester bond, which reduced the hydrophilicity of the surface of the tobacco shreds and diminished their water-holding capacity.

### 3.2.5. Evaluation of the moisture activity of reconstituted tobacco shreds with the addition of target compounds

“Activity of water” was the ratio of the water vapour pressure of a substance to the water vapour pressure of free water at the same temperature. This ratio also indicated the relative humidity of a gas in equilibrium with a substance. In the food industry it referred to the state of moisture in a food product, i.e. The degree to which it was bound to the food or free. The higher the value of water activity, the lower the degree of binding; its value ranged from 0 to 1 (Labuza, 1984). Different states of existence of microscopic water molecules led to differences in the chemical, physical, and biological properties of substances, which were theoretically reflected by water activity and quantified by water

**Table 2**

Fitting results of different models for the desorption of reconstituted tobacco shreds (RH = 32 %, 22 °C).

Sample	Page		Wang and Singh		Henderson-Pabis	
	$R^2$	RMSE	$R^2$	RMSE	$R^2$	RMSE
Glycerol	0.98683	0.000144	0.60075	0.00752	0.94093	0.00065
3a	0.88299	0.00632	0.64611	0.00666	0.93559	0.00359
4a	0.93157	0.00429	0.85106	0.00206	0.95356	0.00359
5a	0.93692	0.00316	0.41995	0.00375	0.91245	0.00438
Control	0.86994	0.00324	0.55655	0.02805	0.83584	0.00137
Glycerol	0.95172	0.000171	0.48525	0.00293	0.8778	0.00576
3b	0.9697	0.0005653	0.45843	0.00965	0.92898	0.00133
4b	0.9194	0.000853	0.85514	0.00136	0.84135	0.00168
5b	0.88741	0.00106	0.86628	0.00682	0.79849	0.0019
Control	0.95272	0.00299	0.73833	0.00137	0.90853	0.00579

**Table 3**

Fitting results for moisture absorption of Page model.

Page	Sample									
	Glycerol	3a	4a	5a	Control	Glycerol	3b	4b	5b	Control
$k$	0.00448	0.00015	0.00345	0.00533	0.00128	0.00205	0.00043	0.000820	0.000469	0.000128
$n$	1.47607	2.2789	1.46898	1.32024	1.6189	1.67611	2.04235	2.35398	2.48347	2.17339

**Table 4**

Fitting results for desorption of Page model.

Page	Sample									
	Glycerol	3a	4a	5a	Control	Glycerol	3b	4b	5b	Control
$k$	0.75159	0.13111	0.04738	0.14754	0.47437	0.76754	0.5318	0.72843	0.7858	0.47437
$n$	0.38187	0.60526	0.79435	0.57853	0.39607	0.52206	0.51868	0.45648	0.44766	0.39607

**Table 5**Half-life mean absorption/desorption rate ( $v$ ), moisture protection index (MPI) and moisture retention index (MRI) of the hygroscopic/descriptive process of reconstituted tobacco shreds different moisturizing agents.

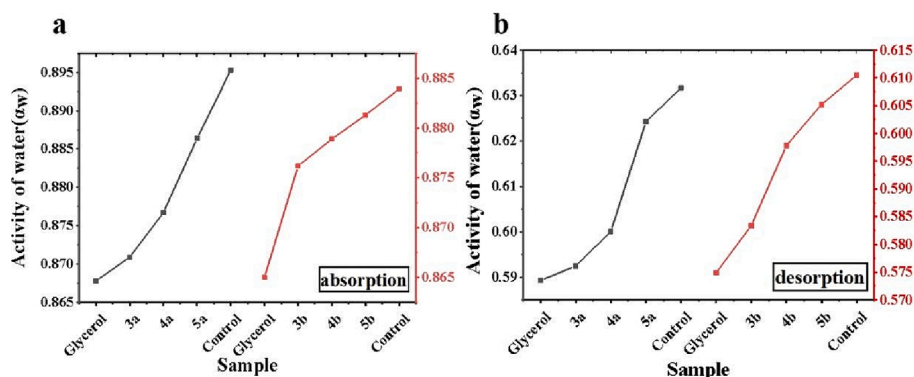
Sample	Absorption		Desorption	
	$v$ (%/h)	MPI	$v$	MRI
Glycerol	0.7245	0.8716	0.01786	2.0435
3a	0.6176	1.3079	0.02037	2.0386
4a	0.4327	2.0646	0.02301	2.0304
5a	0.2879	2.6590	0.02677	2.0254
Control	0.1475	3.2326	0.02692	2.0227
Glycerol	0.6741	1.0713	0.01562	2.0471
3b	0.5749	1.4829	0.01799	2.0459
4b	0.41255	2.1356	0.0217	2.0377
5b	0.3629	2.3426	0.02547	2.0332
Control	0.2415	2.8319	0.0261	2.0315

activity values (Müller & Yamashita, 2008; Obara, Obiedziński & Kołczak, 2006). The water activity of tobacco had a direct impact on its stability during the storage period, therefore, water activity testing was of great importance for tobacco storage.

Fig. 4 showed the water activity ( $a_w$ ) of the tobacco samples with different moisturizing agents added during absorption and desorption. From Fig. 4 the water activity of the tobacco with compounds 3a and 3b differed by about 0.01 % with respect to the ratio of glycerol in both cases. This indicated that 3a and 3b can keep the moisture activity of the tobacco shreds in a relatively low range, so that the water molecules in the tobacco shreds were in a relatively stable state during the preservation period, which reduced the escape ability of the water molecules, thus better maintained the moisture content of the tobacco shreds.

### 3.2.6. Water distribution and migration of reconstituted tobacco shreds with different humectants

The distribution curves of  $T_2$  relaxation times of tobacco with

**Fig. 4.** Activity of water during absorption and desorption of tobacco with different moisturizing agents.

different moisturizing agents at 22 °C, 85 %RH and 33 %RH were shown in Fig. 5 respectively. The different relaxation times reflected the mobility of the moisture and how tightly it was bound to the shredded tobacco. Two distinct H-proton relaxation peaks were observed for all the samples, which represented two different states of moisture. The smaller the value of  $T_2$ , the smaller the degree of free water in the sample, the greater the binding of moisture to the solid matrix, and the poorer the mobility of the sample (Sánchez-Alonso, Moreno & Careche, 2014). On the contrary, the larger the value of  $T_2$ , the greater the amount of free water in the sample, and the higher the mobility of the sample. In general, bound water was water with a relaxation time of less than 1 ms (Li et al., 2012). The corresponding relative areas in Fig. 5 were labelled  $T_{21}$  and  $T_{23}$ , indicating the proportion of bound and free water in the reconstituted tobacco shreds, respectively (Hills, 2006). The size of the peak area represented the amount of water in the corresponding state of existence. A decrease in the peak area was associated with a decrease in water content, while an increase in the peak area is associated with an increase in water content (Wei et al., 2018).

From Fig. 5, the peak of bound water ( $T_{21}$ ) dominated the two states of moisture in different humidity environments (RH = 84 % (a, b), RH = 32 % (c, d)) for the tobaccos spiked with different moisturizing agents, and the proportional content of the two states of moisture was glycerol

> 3a > blank, and glycerol > 3b > blank in both cases. These results could be explained by the fact that glycerol has more hydroxyl groups relative to the synthesized compounds 3a and 3b, thus allowing more hydrogen bonds to be formed between the tobacco and water. This enhanced the bonding between water molecules and the tobacco matrix, facilitated the interaction between the tobacco and water molecules, increased the relative content of bound water, and enhanced the hygroscopicity of the tobacco (Stoilova, Kratchanova & Kratchanov, 1994). Under both high and low RH conditions, the  $T_{21}$  and  $T_{23}$  peaks of the tobacco samples treated with the moisturizing agent showed faster relaxation speeds compared with the control, which indicated that the water presented a denser and more stable state. Moreover, the  $T_{21}$  peak area of sample 3a was higher than that of samples 4a and 5a under both high and low RH conditions, indicating that more moisture was in a bound state in sample 3a, and thus sample 3a had stronger hygroscopicity and water retention. Similarly, sample 3b has stronger hygroscopicity and water retention compared to samples 4b and 5b.

As shown in Fig. 6a and 6c, at 32 % RH and 22 °C, the bound water contents of reconstituted tobacco shreds-glycerol, reconstituted tobacco shreds-3a, reconstituted tobacco shreds-4a, reconstituted tobacco shreds-5a, reconstituted tobacco shreds-3b, reconstituted tobacco shreds-4b, reconstituted tobacco shreds-5b and reconstituted tobacco

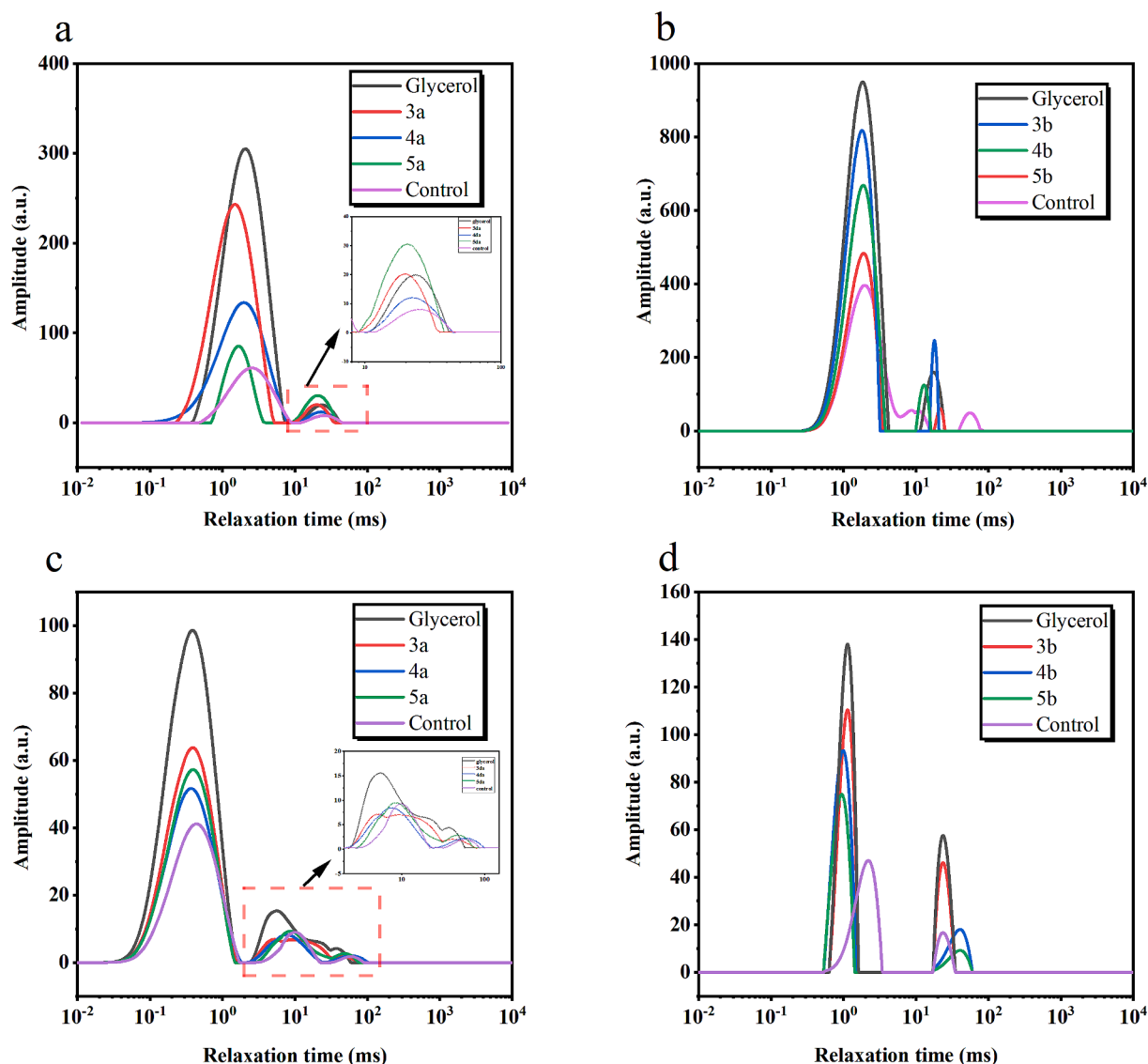


Fig. 5. Transverse relaxation time of reconstituted tobacco shreds at 22 °C, RH = 84 % (a, b), RH = 32 % (c, d).



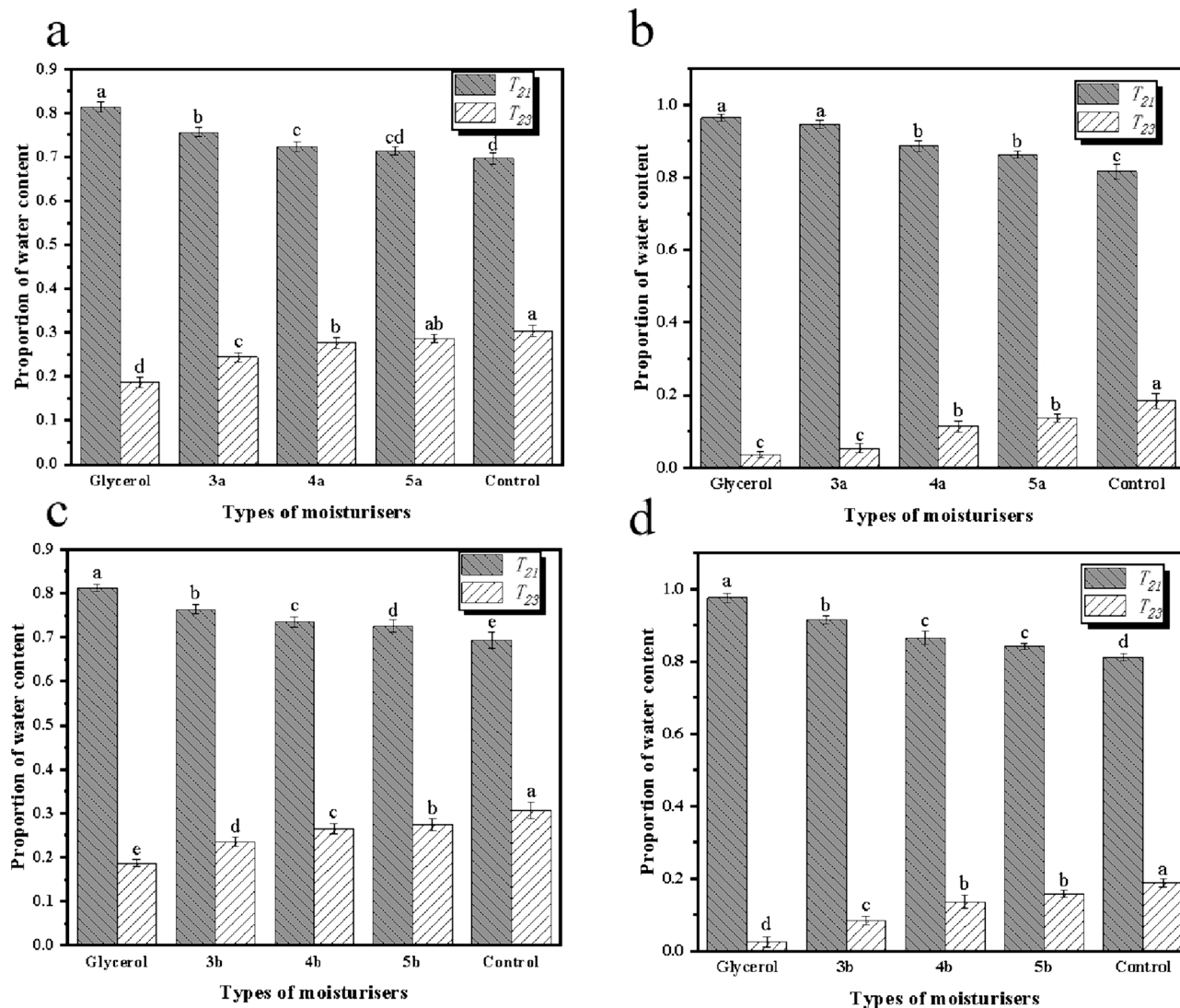


Fig. 6. Proportion of water content of reconstituted tobacco shreds at 22 °C, RH = 32 % (a, c), RH = 84 % (b, d).

shreds control were 0.81236, 0.75639, 0.72571, 0.71179, 0.7654, 0.73624, 0.7291 and 0.69284, respectively. Whereas at 84 % and 22 °C, the bound water contents of these groups were 0.96683, 0.95837, 0.88904, 0.86179, 0.91545, 0.87356, 0.8511 and 0.82179, respectively (Fig. 6b and 6d). These results supported the previous experimental

findings that compounds 3a and 3b could reduce the strong hygroscopicity of glycerol, respectively, while maintaining a certain degree of hygroscopicity and humectancy compared to the control. Therefore, 3a and 3b were selected for subsequent TG-DTG and pyrolysis analysis.

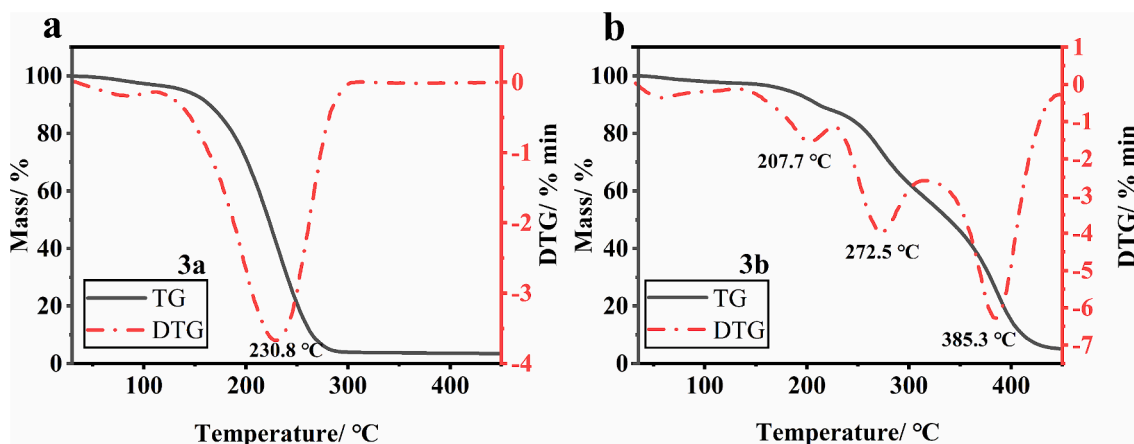


Fig. 7. TG-DTG curves of 3a (a), and 3b (b).

### 3.3. Thermal analysis of 3a and 3b

#### 3.3.1. TG-DTG analysis of 3a and 3b

Thermogravimetric and differential thermogravimetric studies were performed on 3a and 3b to determine the thermal stability of the compounds. Fig. 7a and b showed that during the degradation of compounds 3a and 3b at a heating rate of  $10\text{ }^{\circ}\text{C min}^{-1}$ , compound 3a underwent a major mass change phase between  $147\text{ }^{\circ}\text{C}$  and  $450\text{ }^{\circ}\text{C}$ , with a drastic decrease in mass loss (TG) of 96.49 %. The maximum rate of mass loss occurred at  $230.8\text{ }^{\circ}\text{C}$  with a mass loss of 47.61 %. At this stage, small molecules of solid or liquid material resulting from the degradation of the sample may be further decomposed into gaseous material due to heat absorption.

The main mass change stage of compound 3b occurred between  $187\text{ }^{\circ}\text{C}$  and  $450\text{ }^{\circ}\text{C}$ , and the highest decomposition rate was reached at the peak temperature of  $385.3\text{ }^{\circ}\text{C}$ , with a mass loss rate of 35.46 %. As the temperature increased, the mass loss (TG) of 3b decreased dramatically by 94.83 %. At this point, complex physicochemical changes such as evaporation of water and degradation of compounds may be occurring within the sample. At the end of the mass change phase, the residue was charred at high temperatures. The TG-DTG analysis provided a temperature basis for the analysis of the pyrolysis products of the samples, which could be quantitatively and qualitatively analysed for 3a and 3b in the next experiments.

#### 3.3.2. Pyrolysis analysis of 3a and 3b

Based on the results of TG-DTG analyses, pyrolysis conditions at  $250\text{ }^{\circ}\text{C}$ ,  $300\text{ }^{\circ}\text{C}$  and  $350\text{ }^{\circ}\text{C}$  in atmosphere were designed. And the small molecule pyrolysis products of 3a and 3b were listed respectively. In Table 6, the pyrolysis of 3a at  $250\text{ }^{\circ}\text{C}$  was observed by gas chromatography-mass spectrometry (GC-MS) to yield five products as Glycerol (24.54 %), 1,2,3-Propanetriol, 1-acetate (4.72 %), Triacetin (13.52 %), n-Propyl benzoate (30.35 %), Benzoic acid, 2-methylpropyl ester (16.16 %). Glycerol (45.33 %), 1,2,3-Propanetriol, 1-acetate (6.76 %), n-Propyl benzoate (29.26 %), Benzoic acid, 2-methylpropyl ester (9.01 %) were obtained at  $300\text{ }^{\circ}\text{C}$ . While at  $350\text{ }^{\circ}\text{C}$ , pyrolysis formed Glycerol (40.91 %), 1,2,3-Propanetriol, 1-acetate (5.11 %), n-

Propyl benzoate (39.45 %), Benzoic acid, 2-methylpropyl ester (4.65 %).

In Table 7, the pyrolysis products of 3b at  $250\text{ }^{\circ}\text{C}$  were Glycerol (29.96 %), 1,2,3-Propanetriol, 1-acetate (2.12 %), and 2-Propenoic acid, 3-phenyl-, 2-methylpropyl ester (60.94 %). Benzaldehyde (2.82 %), Glycerol (39.06 %), 1,2,3-Propanetriol, 1-acetate (3.48 %), and 2-Propenoic acid, 3-phenyl-, 2-methylpropyl ester (49.75 %) were obtained at  $300\text{ }^{\circ}\text{C}$ . (49.75 %). However, at  $350\text{ }^{\circ}\text{C}$  pyrolysis formed Benzaldehyde (0.86 %), Glycerol (70.90 %), 1,2,3-Propanetriol, 1-acetate (1.35 %), 2-Propenoic acid, 3-phenyl-, 2-methylpropyl ester (8.90 %).

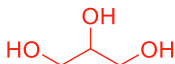
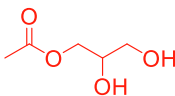
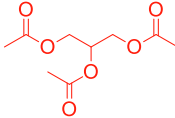
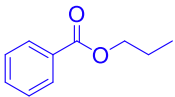
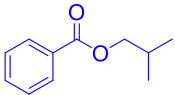
From Tables 6 and 7, the pyrolysis products of 3a and 3b had sweet substances such as n-Propyl benzoate with a nutty and balsamic aroma and a sweet fruity and nutty flavour. Benzoic acid, 2-methylpropyl ester with a sweet and astringent amber aroma and a slightly leafy greenish note with rose, iris and balsamic undertones. 2-Propenoic acid, 3-phenyl-, 2-methylpropyl ester has a sweet fruity and balsamic aroma, like spices, and a creamy sweet amber aroma with hints of cocoa bean and fruity undertones, which are widely used in the food flavouring industry (Taofiq et al., 2017; Chen et al., 2023). Glycerol was the most important parts of all the cleavage products of 3a and 3b. Py-GC/MS studies revealed the correlation between the chemical structure of the samples and the type and content of pyrolysis products. Based on the thermal analysis, the ester bond ( $\text{O}=\text{C}-\text{O}$ ) in the samples may be broken to produce the synthetic substrates, which then decomposes to produce other compounds. The pyrolysis mechanism of 3a and 3b was then deduced.

#### 3.3.3. Pyrolysis mechanism of 3a and 3b

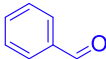
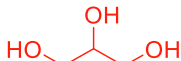
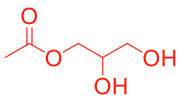
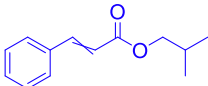
The thermal degradation mechanism of the compounds is very complex, and various reactions such as oxidation, dehydrogenation, addition, rearrangement, and isomerisation may occur at high temperatures, while the pyrolysis temperature influences the relative content of pyrolysis products. The degradation mechanisms of compounds 3a and 3b were preliminarily explored, and their possible cleavage pathways are shown in Fig. 8.

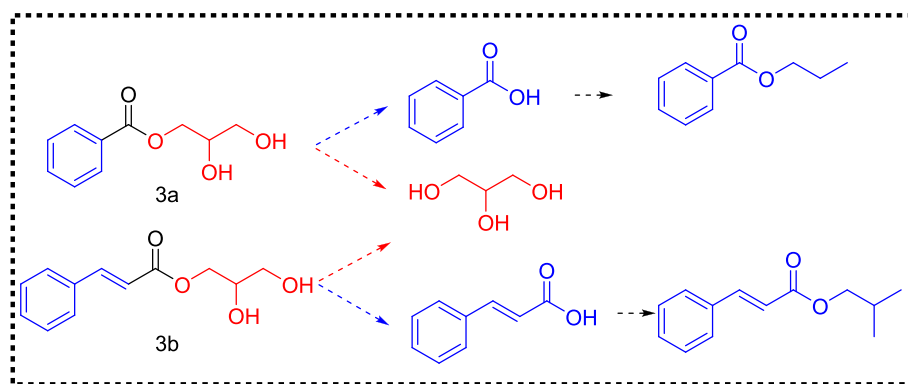
With the increase of pyrolysis temperature, due to the instability of the ester bond  $\text{O}=\text{C}-\text{O}$ , the ester bond in 3a and 3b broke to form glycerol, whereas benzoic acid and cinnamic acid could react with

**Table 6**  
Pyrolysis products of 3a.

Peak	RT/min	Pyrolysis products	Structure	Match	Relative content/%		
					250 °C	300 °C	350 °C
1	8.636	Glycerol		83	24.54 %	45.33 %	40.91 %
2	11.138	1,2,3-Propanetriol, 1-acetate		64	4.72 %	6.76 %	5.11 %
3	16.314	Triacetin		64	13.52 %	–	–
4	29.315	n-Propyl benzoate		59	30.35 %	29.26 %	39.45 %
5	29.657	Benzoic acid, 2-methylpropyl ester		59	17.09 %	9.01 %	4.65 %

**Table 7**  
Pyrolysis products of 3b.

Peak	RT/min	Pyrolysis products	Structure	Match	Relative content/%		
					250 °C	300 °C	350 °C
1	7.435	Benzaldehyde		91	–	2.82 %	0.86 %
2	7.783	Glycerol		88	29.96 %	39.06 %	70.90 %
3	10.904	1,2,3-Propanetriol, 1-acetate		72	2.12 %	3.48 %	1.35 %
4	35.614	2-Propenoic acid, 3-phenyl-, 2-methylpropyl ester		85	60.94 %	49.75 %	18.90 %

**Fig. 8.** Proposed pyrolysis mechanism of 3a and 3b.

various small molecule alcohols to form esters at elevated temperatures. The pyrolysis mechanism of compounds 3a and 3b has been tentatively determined. Because the complexity of the pyrolysis reaction, this speculation needs to be further verified.

#### 4. Conclusions

In summary, six glycerol esters were designed, synthesized and structurally characterized by  $^1\text{H}$  NMR,  $^{13}\text{C}$  NMR, IR and HRMS to verify that the compounds were successfully synthesized. Afterwards, the compounds were subjected to moisture adsorption and retention properties of reconstituted tobacco shreds, model validation, MPI and MRI calculation, water activity, LF-NMR, as well as exploring the thermal behavior of the compounds themselves and deducing their pyrolysis mechanisms. Compared to traditional acid-alcohol esterification reactions, the synthesis of ester derivatives through biological enzyme catalysis offers advantages such as non-pollution, high yield, and environmental friendliness (Fan et al., 2022a, 2022b). The glycerol esters 3a and 3b were found to reduce moisture adsorption to some extent and exhibit moderate moisturizing properties according to the results of moisture adsorption and desorption as well as LF-NMR analysis. This study also investigated, for the first time, the impact of these compounds on the hygroscopic properties of reconstituted tobacco using MPI, MRI, and water activity. According to the TG-DTG results, the total mass loss rates of 3a and 3b were as high as 77.22 % and 89.79 %. During the pyrolysis process, the ester bonds of 3a and 3b were broken to form pyrolysis products, which included raw materials and substrates, such as

glycerol and phenyl ester derivatives, performing the functions of harmonization and reducing the dryness sensation of the smoke. The glycerol esters 3a and 3b in this study had good effect on the reconstituted tobacco moisturizing compared to the traditional moisturizing agents glycerol in the tobacco industry. They could solve the problems of shortened storage time, poor combustibility, and unfavourable smoke flavour during smoking due to the strong hygroscopicity of glycerol in the application of reconstituted tobacco. They were expected to be a new type of moisturizing agent for heating non-combustible tobacco products, but its application safety needs further research.

#### 5. Funding information

China Tobacco Henan Industrial Co., Ltd. (Grant/ Award Number: 2023410001340030); National Natural Science Foundation of China (32300342); Natural Science Foundation of Henan Province (232300421257).

#### CRediT authorship contribution statement

**Ziting Gao:** First draft, revision, editing, Conceptualization, Methodology in writing. **Jiqiang Wan:** Methodology, Investigation. **Lu Han:** Writing first draft, revision, and editing. **Guangming Fu:** Data curation, Investigation. **Xiaopeng Yang:** Methodology. **Qi Guo:** Investigation, Methodology. **Xiaoming Ji:** Formal analysis, Investigation. **Wenjuan Chu:** Data curation, Investigation. **Haiping Tian:** Review & editing, Supervision. **Miao Lai:** Review & editing, Investigation.

## Declaration of competing interest

The authors declare that they have no known competing financial interests or personal relationships that could have appeared to influence the work reported in this paper.

## Acknowledgments

This work was supported by China Tobacco Henan Industrial Co., Ltd. (Grant/ Award Number: 2023410001340030); National Natural Science Foundation of China (32300342); Natural Science Foundation of Henan Province (232300421257).

## References

- Ates, E.G., Domenici, V., Wojciechowska, M.F., et al., 2021. Field-dependent NMR relaxometry for food science: applications and perspectives. *Trends Food Sci. Tech.* 110, 513–524. <https://doi.org/10.1016/j.tifs.2021.02.026>.
- Biaszczyk, N., Rosiak, A., Kałużna-Czaplińska, J., 2021. The potential role of cinnamon in human health. *Forests*. 12 (5), 648. <https://doi.org/10.3390/f12050648>.
- Cebrián-Tarancon, C., Fernández-Roldán, F., Sánchez-Gómez, R., et al., 2022. Pruned vine-shoots as a new enological additive to differentiate the chemical profile of wines. *Food Res. Int.* 156, 111195 <https://doi.org/10.1016/j.foodres.2022.111195>.
- Chen, J.H., Zhang, Y., Zhong, H.Y., et al., 2023. Efficient and sustainable preparation of cinnamic acid flavor esters by immobilized lipase microarray. *LWT* 173, 114322. <https://doi.org/10.1016/j.lwt.2022.114322>.
- Fan, W.P., Chu, W.J., Li, Y.G., et al., 2022a. Synthesis, characterization and thermal behavior of n-substituted pyrrole esters. *ChemistrySelect*. 44 (7), e202203722.
- Fan, W.P., Chu, W.J., Tian, H.Y., et al., 2022b. Synthesis and pyrolysis of two novel pyrrole ester flavor precursors. *J. Heterocyclic Chem.* 59 (8), 1397–1406. <https://doi.org/10.1002/jhet.4479>.
- Fan, W.P., Tian, H.Y., Chen, H.L., et al., 2023. Moisture property and thermal behavior of two novel synthesized polyol pyrrole esters in tobacco. *ACS Omega*. 8 (5), 4716–4726. <https://doi.org/10.1021/acsomega.2c06683>.
- Gao, Z.T., Chu, W.J., Han, L., et al., 2023. Analysis of hygroscopicity and pyrolysis behaviour of propanediol esters synthesized by the enzymatic method. *Flav. Fragr. J.* 39, 125–135. <https://doi.org/10.1002/ffj.3771>.
- Grajales-Hernández, D., Armendariz-Ruiz, M., Gallego, F.L., Mateos-Díaz, J., 2021. Approaches for the enzymatic synthesis of alkyl hydroxycinnamates and applications thereof. *Appl. Microb. Biot.* 105 (10), 3901–3917. <https://doi.org/10.1007/s00253-021-11285-z>.
- Gunia-Krzyzak, A., Sloczynska, K., Popiol, J., et al., 2018. Cinnamic acid derivatives in cosmetics: current use and future prospects. *Int. J. Cosmetic Sci.* 40, 356–366. <https://doi.org/10.1111/ics.12471>.
- Heck, J.D., Gaworski, C.L., Rajendran, N., et al., 2002. Toxicologic evaluation of humectants added to cigarette tobacco: 13-week smoke inhalation study of glycerin and propylene glycol in fischer 344 rats. *Inhal Toxicol.* 14 (11), 1135–1152. <https://doi.org/10.1080/08958370290084827>.
- Hills, B., 2006. Applications of low-field NMR to food science. *Annu. Rep. NMR Spectro.* 58 (5), 177–230. [https://doi.org/10.1016/S0066-4103\(05\)58004-9](https://doi.org/10.1016/S0066-4103(05)58004-9).
- Hu, X.Y., Wu, P., Zhang, S.P., Chen, S., Wang, L., 2018. Moisture conversion and migration in single-wheat kernel during isothermal drying process by LF-NMR. *Dry Technol.* <https://doi.org/10.1080/07373937.2018.1459681>.
- Huang, Y., Du, G., Ma, Y., Zhou, J., 2021. Predicting heavy metals in dark sun-cured tobacco by near-infrared spectroscopy modeling based on the optimized variable selections. *Ind. Crops Prod.* 172, 114003 <https://doi.org/10.1016/j.indcrop.2021.114003>.
- Ih, O., Gr, J., 2014. Diffusion of moisture in a cigarette tobacco column at room conditions. *Contrib. Tob. Res.* 21 (1), 15–24.
- Johnson, W., Bergfeld, W.F., Belsito, D.V., et al., 2017. Safety assessment of benzyl alcohol, benzoic acid and its salts, and benzyl benzoate. *Int. J. Toxicol.* 36 (3), 5S–30S. <https://doi.org/10.1177/1091581817728996>.
- Labuza, T.P., 1984. Application of chemical kinetics to deterioration of foods. *J. Chem. Educ.* 61 (4), 348. <https://doi.org/10.1021/ed061p348>.
- Lachenmeier, D.W., Anderson, P., Rehm, J., 2018. Heat-not-burn tobacco products: the devil in disguise or a considerable risk reduction? *Int. J. Alcoh. Drug Res.* 7 (2), 8–11. <https://doi.org/10.7895/ijadr.250>.
- Li, X., Ma, L.Z., Tao, Y., et al., 2012. Low field-NMR in measuring water mobility and distribution in beef granules during drying process. *Adv. Mater. Res.* 550, 3406–3410.
- Lin, C., Cui, H.P., Wang, X.J., et al., 2020. Regulating water binding capacity and improving porous carbohydrate matrix's humectant and moisture proof functions by mixture of sucrose ester and *Polygonatum sibiricum* polysaccharide. *Int. J. Biol. Macromol.* 147 <https://doi.org/10.1016/j.ijbiomac.2020.01.101>.
- Müller, C.M.O., Yamashita, F., 2008. Evaluation of the effects of glycerol and sorbitol concentration and water activity on the water barrier properties of cassava starch films through a solubility approach. *Carbohydr. Polym.* 72 (1), 82–87. <https://doi.org/10.1016/j.carbpol.2007.07.026>.
- Mutasa, E.S., Seal, K.J., Magan, N., 1990. The water-content water activity relationship of cured tobacco and water relations of associated spoilage fungi. *Int. Biodeterior.* 26 (6), 381–396.
- Obara, A., Obiedziński, M., Kolczak, T., 2006. The effect of water activity on cholesterol oxidation in spray and freeze-dried egg powders. *Food Chem.* 95 (2), 173–179. <https://doi.org/10.1016/j.foodchem.2004.06.021>.
- Pan, H., Lu, T., Wu, X., Jiang, C., Jin, J., 2019. Synthesis of C-ring hydrogenated sinomenine cinnamate derivatives via Heck reactions. *J. Chem. Res.* 43 (11–12), 469–473. <https://doi.org/10.1177/1747519819868201>.
- Prakash, B., Singh, P., Mishra, P.K., Dubey, N.K., 2012. Safety assessment of *Zanthoxylum alatum* Roxb. essential oil, its antifungal, anti-aflatoxin, antioxidant activity and efficacy as antimicrobial in preservation of *Piper nigrum* L. fruits. *Int. J. Food Microbiol.* 153 (1–2), 183–191. <https://doi.org/10.1016/j.ijfoodmicro.2011.11.007>.
- Qin, C., Du, Y., Xiao, L., Liu, Y., Yu, H., 2002. Moisture retention and antibacterial activity of modified chitosan by hydrogen peroxide. *J. Appl. Polym. Sci.* 86, 1724–1730. <https://doi.org/10.1002/app.11080>.
- Rainey, C.L., Shifflett, J.R., Goodpaster, J.V., et al., 2013. Quantitative analysis of humectants in tobacco products using gas chromatography (GC) with simultaneous mass spectrometry (MSD) and flame ionization detection (FID). *Contrib. Tobacco Res.* 25 (6), 576–585.
- Samejima, T., Soh, Y., Yano, T., 1978. Moisture sorption isotherms of various tobaccos. *Agric. Biol. Chem.* 42 (12), 2285–2290.
- Samejima, T., Yano, T., 1985. Moisture diffusion within shredded tobacco leaves. *Agric. Biol. Chem.* 49 (6), 1809–1812.
- Sánchez-Alonso, I., Moreno, P., Careche, M., 2014. Low field nuclear magnetic resonance (LF-NMR) relaxometry in hake muscle after different freezing and storage conditions. *Food Chem.* 153 (15), 250–257. <https://doi.org/10.1016/j.foodchem.2013.12.060>.
- Simonaciuc, E., McNeill, A., Shahab, L., et al., 2019. Heat-not-burn tobacco products: a systematic literature review. *Tob. Control.* 28 (5), 582–594. <https://doi.org/10.1136/tobaccocontrol-2018-054419>.
- Stoilova, A., Kratchanova, M., Kratchanov, C., 1994. Comparative investigations of the influence of polyalcohol and fruit extracts on the physicochemical properties of tobacco. *Contrib. Tobacco Res.* 16 (1), 1–9.
- Tani, H., Hikami, S., Takahashi, S., et al., 2019. Isolation, identification, and synthesis of a new prenylated cinnamic acid derivative from Brazilian green propolis and simultaneous quantification of bioactive components by LC-MS/MS. *J. Agric. Food Chem.* 67 (44), 12303–12312. <https://doi.org/10.1021/acs.jafc.9b04835>.
- Taofiq, O., González-Parrañas, A.M., Barreiro, M.F., Fe Rreira, I.C.F.R., 2017. Hydroxycinnamic acids and their derivatives: cosmecutaneous significance, challenges and future perspectives, a review. *Molecules*. 22 (2), 281. <https://doi.org/10.3390/molecules22020281>.
- Wang, J., Jin, W., Hou, Y., et al., 2013. Chemical composition and moisture-absorption/retention ability of polysaccharides extracted from five algae. *Int. J. Biol. Macromol.* 57, 26–29. <https://doi.org/10.1016/j.ijbiomac.2013.03.001>.
- Wei, S., Tian, B., Jia, H., et al., 2018a. Investigation on water distribution and state in tobacco leaves with stalks during curing by LF-NMR and MRI. *Dry Technol.* 36 (4), 1–8. <https://doi.org/10.1080/07373937.2017.1415349>.
- Wei, S., Tian, B.Q., Jia, H.F., et al., 2018b. Investigation on water distribution and state in tobacco leaves with stalks during curing by LF-NMR and MRI. *Dry Technol.* 36 (12), 1515–1522. <https://doi.org/10.1080/07373937.2017.1415349>.
- Wenda, S., Illner, S., Mell, A., Kragl, U., 2011. Industrial biotechnology—the future of green chemistry. *Green Chem.* 13 (11), 3007–3047. <https://doi.org/10.1039/C1GC15579B>.
- Xiang, X.F., Lan, Y.B., Gao, X.T., et al., 2020. Characterization of odor-active compounds in the head, heart, and tail fractions of freshly distilled spirit from Spine grape (*Vitis davidii* Foex) wine by gas chromatography-olfactometry and gas chromatography-mass spectrometry. *Food Res. Int.* 137, 109388 <https://doi.org/10.1016/j.foodres.2020.109388>.
- Yang, S., Liu, J.S., Zheng, M.Z., et al., 2019. Effect of fermentation on water mobility and distribution in fermented cornmeal using LF-NMR and its correlation with substrate. *J. Food. Sci. Technol.* 56 (2), 1027–1036. <https://doi.org/10.1007/s13197-019-03569-0>.
- Yin, C.Y., Xu, Z.Q., Shu, J.S., et al., 2015. Influence of physico-chemical characteristics on the effective moisture diffusivity in tobacco. *Int. J. Food Prop.* 18 (3), 690–698. <https://doi.org/10.1080/10942912.2013.845785>.
- Zhao, Q.R., Wang, L.X., Chen, H.R., et al., 2023. Enzyme-catalyzed synthesis, odor characteristics and thermal analysis of new pyridine esters. *ChemistrySelect* 8 (10), e202204356.
- Zhou, C.F., Qian, P., Meng, J., et al., 2016. Effect of glycerol and sorbitol on the properties of dough and white bread. *Cereal Chem.* 93 (2), 196–200. <https://doi.org/10.1094/CCHEM-04-15-0087-R>.